PROCEEDINGS OF SCIENCE

Dispersive determinations of lattice HVP window quantities for muon $g-2$

Kim Maltman,[a,b,*] **Genessa Benton,**[c] **Diogo Boito,**[d] **Maarten Golterman,**[e] **Alexander Keshavarzi**[f] **and Santiago Peris**[g]

[a] *Department of Mathematics and Statistics, York University, 4700 Keele St, Toronto, Canada M3J 1P3*
[b] *CSSM, University of Adelaide, Adelaide, SA 5005, Australia*
[c] *Department of Physics, University of Illinois, Urbana, IL 61801, USA*
[d] *Instituto de Física de São Carlos, Universidade de São Paulo, 13560-970, São Carlos, SP, Brazil*
[e] *Department of Physics and Astronomy, San Francisco State University, San Francisco, CA 94132, USA*
[f] *Department of Physics and Astronomy, University of Manchester, Manchester M13 9PL, United Kingdom*
[g] *Department of Physics and IFAE-BIST, Universitat Autònoma de Barcelona, E-08193 Bellaterra, Barcelona, Spain*
E-mail: kmaltman@yorku.ca, gbenton@sfsu.edu, boito@ifsc.usp.br, maarten.golterman@gmail.com, alex.i.keshavarzi@gmail.com, peris@ifae.es

We report on recent dispersive determinations of contributions to $a_\mu^{\rm HVP}$, the hadronic vacuum polarization contribution to the anomalous magnetic moment of the muon. The results provide data-driven determinations of components which are separately calculated and summed to produce the alternate lattice determination, with the goal of clarifying the region (or regions) in the dispersive spectrum responsible for recently observed discrepancies between lattice and dispersive results. Dispersive results are presented for the isospin-limit, light-quark-connected (lqc) and strange-connected-plus-full-*uds*-disconnected (s+lqd) components of, in addition to $a_\mu^{\rm HVP}$ itself, various "windowed" versions thereof. The discrepancy between lattice and dispersive results is shown to lie almost entirely in the lqc component, and to be largest for those observables that weight most heavily contributions from the ρ peak region. We also show that all the observed discrepancies are removed if, in the dispersive determinations, recently released CMD-3 results for the $e^+e^- \to \pi^+\pi^-$ cross sections are used, in the region covered by the CMD-3 data, in place of the combination of results from previous experiments employed in the 2020 $g-2$ Theory Initiative white paper assessment.

The XVIth Quark Confinement and the Hadron Spectrum Conference (QCHSC24)
19-24 August, 2024
Cairns Convention Centre, Cairns, Queensland, Australia

*Speaker

 ISSN 1824-8039 . Published by SISSA Medialab.

PoS(QCHSC24)178

1. Introduction

Results from BNL E821 [1] and Runs 1 and 2/3 of the Fermilab E989 [2–4] $g-2$ experiment have reduced the error on a_μ, the anomalous magnetic moment of the muon, to the 0.19 ppm level, with a further reduction to $\sim$ 0.14 ppm expected from the soon-to-be-released E989 Run 4/5 analysis. Theoretical efforts are ongoing to achieve a comparable precision for the Standard Model (SM) expectation and take advantage of this improved experimental situation. The dominant source of uncertainty on the SM expectation is currently $a_\mu^{\rm HVP}$, the hadronic vacuum polarization (HVP) contribution, which can be evaluated either dispersively (as a weighted integral over inclusive $e^+e^- \to$ hadrons cross-sections), or on the lattice. A review of the status of these determinations as of 2020, with a final assessment relying on the at-that-time-more-precise dispersive determination, can be found in the $g-2$ Theory Initiative whitepaper [5] (WP1). The SM prediction for a_μ employing that assessment differs from the BNL result by $3.7\,\sigma$, from the post-E989-Run 1 world average by $4.2\,\sigma$, and from the post-E989-Run 2/3 world average by $5.0\,\sigma$.

The first lattice $a_\mu^{\rm HVP}$ result with sub-% precision, by the BMW collaboration [8], was posted too late to be included in the WP1 assessment. Its larger $a_\mu^{\rm HVP}$ produced an associated SM a_μ prediction within $\sim 1\sigma$ of the experimental average. Subsequent lattice studies, including those of "windowed" quantities involving different weightings of the dispersive spectrum, confirm the existence of significant discrepancies between lattice and WP1-assessment-based dispersive determinations. The situation is further complicated by recent CMD-3 results for the $e^+e^- \to \pi^+\pi^-$ cross sections [9], which are significantly larger than those entering the WP1 assessment in the ρ peak region.

The lattice determination of $a_\mu^{\rm HVP}$ typically involves a number of individual, separately calculated contributions, characterized by quark flavor and quark-line connectivity/disconnectivity. The largest of these, in order of size, are the isospin-limit ud (light-quark) connected, the isospin-limit s-quark connected and three-flavor uds disconnected components. Additional smaller contributions come from charm and bottom quarks and from electromagnetic (EM) and strong-isospin-breaking (SIB) corrections, which are treated, respectively, to first order in α and $m_d - m_u$. A more detailed exploration of the lattice-dispersive discrepancy requires dispersive evaluations of as many of these contributions as possible. In what follows, we describe how this can be accomplished, focusing on the dominant 3-flavor (uds) sector.

2. Background and analysis strategy

The master formula for the dispersive (data-driven) evaluation of $a_\mu^{\rm HVP}$ is [6]

$$a_\mu^{\rm HVP} = \frac{4\alpha^2 m_\mu^2}{3} \int_{m_{\pi^0}^2}^{\infty} ds\, \frac{\hat{K}(s)}{s^2} \rho_{\rm EM}(s)\,, \tag{1}$$

with $\hat{K}(s)$ a known, slowly varying, monotonically increasing function and $\rho_{\rm EM}(s)$ the spectral function of the EM hadronic-current vacuum polarization, related to the measured R ratio by $\rho_{\rm EM}(s) = R(s)/12\pi^2$. $R(s)$ is typically obtained as a sum over exclusive-mode contributions up to a point $s = s_{\rm excl}$, with $s_{\rm excl} \sim 4$ GeV^2, and from inclusive data, plus narrow exclusive charm and

bottom resonance contributions, above that. Windowed versions, $a_\mu^{W,\mathrm{HVP}}(s)$, can be obtained by inserting the relevant weight factor $W(s)$ into the integrand of Eq. (1).

Recent lattice determinations of a_μ^{HVP} employ the related time-momentum form

$$a_\mu^{\mathrm{HVP}} = 2\int_0^\infty dt\, w(t) C(t), \tag{2}$$

with t the Euclidean time, $w(t)$ a known function related to $\hat{K}(s)$, and $C(t)$ the zero-momentum version of the time-momentum representation of the EM current-current two-point function [7], related, for $t > 0$, to $\rho_{\mathrm{EM}}(s)$ by

$$C(t) = \int_0^\infty d(\sqrt{s})\rho_{\mathrm{EM}}(s)\, s\, e^{-\sqrt{s}t}\,. \tag{3}$$

The representation Eq. (2) can also be split into a sum of the short-, intermediate- and long-distance "window" contributions, $a_\mu^{\mathrm{SD,int,LD}}$, proposed by RBC/UKQCD [10], obtained by inserting, the factors $1-\theta(t,t_0,\Delta)$, $\theta(t,t_0,\Delta)-\theta(t,t_1,\Delta)$ and $\theta(t,t_1,\Delta)$, respectively, with

$$\theta(t,t',\Delta) = \frac{1}{2}\left[1+\tanh\left(\frac{t-t'}{\Delta}\right)\right], \tag{4}$$

into the integrand of Eq. (2). The corresponding dispersive representations are obtained by substituting Eq. (3) into the windowed versions of Eq. (2). The choice $t_0 = 0.4$ fm, $t_1 = 1.0$ fm and $\Delta = 0.15$ fm produces the widely studied original RBC/UKQCD windows, and the alternate choice, $t_0 = 1.5$ fm, $t_1 = 1.9$ fm and $\Delta = 0.15$ fm, the larger-t- (smaller-s)-focused intermediate window, W2, introduced in Ref. [11]. The RBC/UKQCD and W2 windows involve dispersive weights which are still largest at low s. Additional window quantities, $I_{\hat{W}_{15}}$ and $I_{\hat{W}_{25}}$, constructed in Ref. [12] from linear combinations of the RHSs of Eq. (3) at a finite set of judiciously chosen t, provide further alternatives without this low-s enhancement.

The decomposition of the uds quark part of the EM current into its $I = 1$ and $I = 0$ ($SU(3)_F$ labels 3, 8) components, produces associated decompositions of $\rho_{\mathrm{EM}}(s)$, $C(t)$ and weighted integrals thereof into pure $I = 1$ (flavor 33), pure $I = 0$ (flavor 88) and mixed-isospin (flavor 38, MI) components. In the isospin limit (i) the MI component vanishes, (ii) the $I = 1$ component is pure light-quark connected (lqc) and (iii) the $I = 0$ component contains a lqc contribution one-ninth the size of the $I = 1$ contribution and the "s+lqd" sum of the strange-quark connected and all uds quark disconnected contributions. The lqc and s+lqd components of $\rho_{\mathrm{EM}}(s)$ in this limit are thus

$$\begin{aligned}\rho^{\mathrm{lqc}}(s) &= \frac{10}{9}\rho_{\mathrm{EM}}^{\mathrm{I=1}}(s)\,,\\ \rho^{\mathrm{s+lqd}}(s) &= \rho_{\mathrm{EM}}^{\mathrm{I=0}}(s) - \frac{1}{9}\rho_{\mathrm{EM}}^{\mathrm{I=1}}(s)\,,\end{aligned} \tag{5}$$

allowing the separate lqc and s+lqd contributions to any weighted spectral integral to be obtained once the $I = 1$ and $I = 0$ components of $\rho_{\mathrm{EM}}(s)$ have been identified. We discuss below the strategies to accomplish this separation in the regions where inclusive and sum-over-exclusive-mode determinations of $R(s)$ are employed. Beyond the isospin limit, $O(m_d - m_u)$ SIB contributions are purely MI, while $O(\alpha)$ EM contributions appear in all of the 33, 88 and 38 components.

In the region where inclusive $R(s)$ data is used, measured $R(s)$ values are well approximated by perturbative QCD (pQCD). With the latter being 75% $I = 1$ and 25% $I = 0$, the $I = 1/0$ separation is trivial for this dominant contribution. Integrated versions of possible small duality-violating (DV) deviations from pQCD allowed by the data are handled using the results of the DV studies of Refs. [13, 14], and turn out to be numerically very small.

In the exclusive-mode region, the $I = 1/0$ separation is straightforward for modes with positive (negative) G-parity (collectively "unambiguous modes") which have $I = 1$ (0). The less straightforward separation for contributions from modes which are not G-parity eigenstates ("ambiguous modes") is discussed in more detail below. We employ first the exclusive-mode data used in the WP1 assessment, but also investigate the impact of replacing with recent CMD-3 $\pi\pi$ results [9] the $\pi\pi$ part of that input from the region 0.33 to 1.2 GeV covered by the CMD-3 data. The CMD-3 study is exploratory only since it is not currently known how to resolve the discrepancies between CMD-3 and earlier $\pi\pi$ results. "KNT19" inputs (2019 versions of the exclusive-mode distributions and covariances provided by the KNT collaboration [15]) are used to evaluate all weighted exclusive-mode integrals. The upper limit of the integration range in this case is $s_{\rm excl} = (1.937\ {\rm GeV})^2$. Alternate $a_\mu^{\rm HVP}$ results based on the $s_{\rm excl} = (1.8\ {\rm GeV})^2$ exclusive-mode $a_\mu^{\rm HVP}$ integrals reported in Ref. [16] (DHMZ) are also presented. DHMZ-based results have not been computed for the windowed observables or the CMD-3-modified $a_\mu^{\rm HVP}$ case since DHMZ versions of the exclusive-mode distribution information needed to calculate them are not publicly available.

Ambiguous mode contributions, which constitute 7% of the KNT19 exclusive-mode $a_\mu^{\rm HVP}$ total, are of two types: those for which the $I = 1/0$ separation can be accomplished using external, non-G-parity-based input, and those for which this is not possible. For the latter, we employ the following "maximally conservative" strategy. Given a specific exclusive mode, X, the positivity of the $I = 1$ and 0 components of $[\rho_{\rm EM}(s)]_X$, the mode-X contribution to $\rho_{\rm EM}(s)$, ensures the corresponding mode-X lqc and s+lqd combinations lie in the ranges $(5/9 \pm 5/9)\ [\rho_{\rm EM}(s)]_X$ and $(4/9 \pm 5/9)\ [\rho_{\rm EM}(s)]_X$, respectively [17], with exactly analogous bounds for the lqc and s+lqd combinations of ambiguous-mode contributions to weighted integrals involving weights which are ≥ 0 for all s. Fortunately, contributions to the various weighted integrals from modes where this assessment must be used are small. The associated uncertainties are therefore also small, sufficiently so on the scale of other errors. This would not be true for the largest of the ambiguous-mode contributions, especially that of $K\bar{K}$ (which, e.g., represents $\sim 80\%$ of the total ambiguous-mode contribution to $a_\mu^{\rm HVP}$) where the maximally conservative version of the uncertainty would swamp all other errors. Luckily, external information is available in all such cases.

For the $K\bar{K}$ mode, BaBar results for the differential $\tau \to K^0 K^- \nu_\tau$ distribution [18], combined with CVC, provide (up to negligible isospin-breaking (IB) corrections) a determination of the $I = 1$ component of $[\rho_{\rm EM}(s)]_{K\bar{K}}$ in the region, $s \leq 2.7556\ {\rm GeV}^2$, responsible for a large fraction of the full unseparated $K\bar{K}$ total. The $K\bar{K}$ separation in this region is thus very precise. The separation in the remainder of the KNT19 exclusive-mode region, where $K\bar{K}$ contributions are much smaller, is handled using the maximally conservative prescription. As expected given the large ϕ peak in $[\rho_{\rm EM}(s)]_{K\bar{K}}$, the $I = 0$ component dominates $K\bar{K}$ contributions to the various weighted integrals, and plays an important role in determinations of the s+lqd components. Use of τ input reduces the uncertainty on the $K\bar{K}$ contributions to these s+lqd quantities by a factor of $\sim 40 - 60$ relative to those obtainable using only the maximally conservative prescription.

The next largest of the ambiguous-mode contributions is that of the radiative mode $\pi^0\gamma$. With contributions from this mode already IB, the MI component is, in general, no longer suppressed, and a full $I = 1/I = 0$/MI separation is required. Here one can take advantage of the strong dominance of the $e^+e^- \to \pi^0\gamma$ cross sections by contributions from intermediate vector-mesons. The associated $V = \rho,\ \omega,\ \phi$ contributions to the amplitude are determined by the V-EM-current and $V - \pi^0\gamma$ couplings, whose magnitudes are fixed by the measured $\Gamma[V \to e^+e^-]$ and $\Gamma[V \to \pi^0\gamma]$ widths. Up to contributions higher order in IB, the ρ contribution to the amplitude is pure isovector and the ω and ϕ contributions pure isoscalar. The $I = 1$, $I = 0$ and MI contributions to the cross sections, and hence to $R(s)$ and the various weighted integrals thereof, are thus obtained from the squared modulus of the ρ contribution, the squared modulus of the sum of ω and ϕ contributions, and the interference between the ρ and ω+ϕ contributions, respectively. With the $e^+e^- \to \eta\gamma$ cross sections similarly dominated by intermediate vector-meson contributions, the $I = 1/I = 0$/MI separation of the smaller radiative $\eta\gamma$ mode contributions can be similarly performed. Further details of the separation for these modes can be found in Appendix B of Ref. [19].

The third largest ambiguous-mode contribution is that of the $K\bar{K}\pi$ modes. Here we employ the already existing separation of the $e^+e^- \to K\bar{K}\pi$ cross sections into $I = 1$ and 0 components produced by the BaBar Dalitz plot analysis of Ref. [20]. This again provides a dramatic reduction in the uncertainties on those components relative to what would be achieved using the maximally conservative prescription.

The final ingredient required before comparing dispersive results to their isospin-limit lattice counterparts is an assessment of the IB contributions still present in the dispersive results obtained using the procedures detailed above. To first order in IB, these come in the form of either MI, 38, "contaminations" (both EM and SIB) present in the nominally pure 33 and 88 components obtained above or EM contributions to the actual 33 and 88 components. Examples of the former are the ρ-ω interference contributions to the 2π and 3π electroproduction cross sections, which, before IB corrections are applied, are assigned to the 33 and 88 components. Because of the $I = 1/0$ separation employed when determining lqc and s+lqd components, these MI contaminations must be identified and subtracted exclusive mode by exclusive mode, though there is no need to separate the individual EM and SIB components. In contrast, no separation into individual exclusive-mode contributions is required for the EM corrections to the actual 33 and 88 components.

We expect the dominant MI EM+SIB contaminations to be those present in the nominally 33 2π and nominally 88 3π contributions, which are strongly enhanced by ρ-ω interference. These have been determined, for $a_\mu^{\rm HVP}$ and a number of window quantities, including the original RBC/UKQCD windows, in the dispersively improved 2π and 3π analyses of Refs. [21, 22]. For the remaining exclusive modes, where no evaluations of the MI contamination exist, but also no enhancements of IB by narrow nearby resonance interference are anticipated, we assign an additional MI-contamination-induced uncertainty equal to 1% of the corresponding exclusive-mode contribution. To be conservative, these are treated as 100% correlated, and added linearly.

Currently, purely dispersive determinations do not appear feasible for the inclusive 33 and 88 EM corrections. While dispersive evaluations exist for some enhanced EM contributions [23], strong cancellations exist among these and it is not known how to obtain estimates for additional contributions which, given these cancellations, may not be numerically negligible (for an expanded discussion of this point, see Ref. [24]). We thus rely, where possible, on inclusive EM lattice results

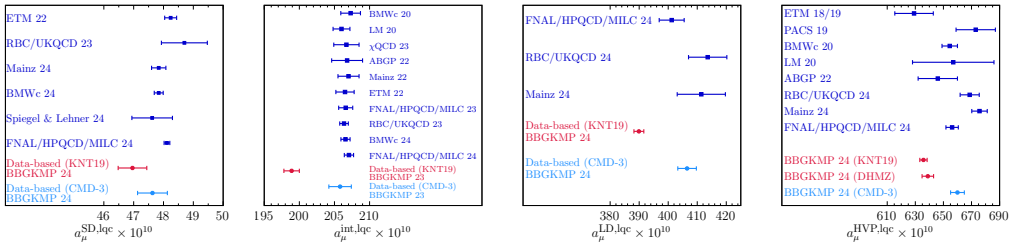

Figure 1: Isospin-symmetric lattice and dispersive results for the lqc components of a_μ^{HVP} and the RBC/UKQCD windows. First panel: dispersive [26] and lattice [37, 39–42, 45] results for $a_\mu^{\mathrm{SD,lqc}}$. Second panel: dispersive [19, 25] and lattice [8, 11, 34–39, 45] results for $a_\mu^{\mathrm{int,lqc}}$. Third panel: dispersive [26] and lattice [43, 44, 46] results for $a_\mu^{\mathrm{LD,lqc}}$. Fourth panel: dispersive [24, 26] and lattice [8, 11, 29–34, 43, 46] results for $a_\mu^{\mathrm{HVP,lqc}}$.

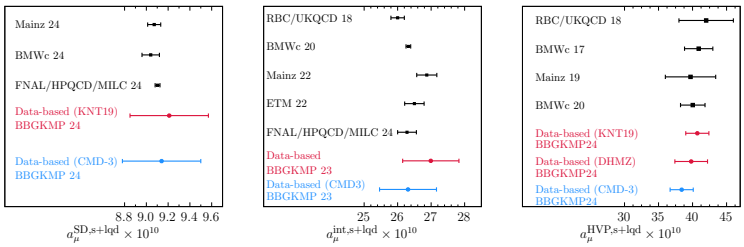

Figure 2: Isospin-symmetric lattice and dispersive results for the s+lqd components of $a_\mu^{\mathrm{SD,s+lqd}}$, $a_\mu^{\mathrm{int,s+lqd}}$ and $a_\mu^{\mathrm{HVP,s+lqd}}$. First panel: dispersive [26] and lattice [40, 41, 45] results for $a_\mu^{\mathrm{SD,s+lqd}}$. Second panel: dispersive [19, 26] and lattice [8, 10, 36, 37, 45] results for $a_\mu^{\mathrm{int,s+lqd}}$. Third panel: dispersive [17, 19, 26] and lattice [8, 10, 27, 28, 33] results for $a_\mu^{\mathrm{HVP,s+lqd}}$. No lattice results currently exist for $a_\mu^{\mathrm{LD,s+lqd}}$.

reported by BMW [8, 41], which correspond to the EM/SIB separation prescription in which both charged and neutral pions have the experimental neutral pion mass in the isospin limit. Conservative estimates are used for the SD and LD window cases, where the required lattice EM inputs are not available. The resulting EM corrections turn out to be very small for all quantities considered. Further details of our treatment of EM corrections can be found in Refs. [17, 19, 24–26].

3. Results

Comparisons of our dispersive determinations (labelled "BBGKMP 24") with recent lattice results are provided for (i) the isospin-limit lqc components of a_μ^{HVP}, a_μ^{SD}, a_μ^{int} and a_μ^{LD} in Fig. 1, and (ii) the s+lqd components of a_μ^{HVP}, a_μ^{SD} and a_μ^{int} in Fig. 2. Dispersive results plotted in red were obtained using KNT19 (alternately DHMZ, for $a_\mu^{\mathrm{HVP,lqc}}$ and $a_\mu^{\mathrm{HVP,s+lqd}}$ only) exclusive-mode input, while those plotted in cyan come from the exploratory study in which CMD-3 $\pi\pi$ data replaces KNT19 $\pi\pi$ data in the region 0.33 GeV $\leq \sqrt{s} \leq$ 1.2 GeV and KNT19 data are used for all other exclusive mode input. The corresponding lattice results are plotted in the upper portion of each panel.

Figure 1 shows clear discrepancies between dispersive results calculated using pre-CMD-3 $\pi\pi$ data and the corresponding lattice determinations. These discrepancies are largest for $a_\mu^{\rm int,lqc}$, which most heavily weights the ρ peak region of the dispersive spectrum, and smallest for $a_\mu^{\rm SD,lqc}$, which least heavily weights that region. Figure 2 shows, in contrast, good agreement between lattice and dispersive determinations for the s+lqd components. The exploratory study employing CMD-3 $\pi\pi$ data, which has larger cross sections in the ρ peak region, shows that use of the CMD-3 data removes all of the observed lqc lattice-dispersive discrepancies without spoiling the good agreement for the s+lqd components. All of the above observations also hold for the W2 intermediate window and the alternate intermediate window quantities, $I_{\hat{W}_{15}}$ and $I_{\hat{W}_{25}}$, which weight even more specifically the ρ peak region. Numerical versions of the results shown in the figures, as well as for the W2 and $I_{\hat{W}_{15}}$ and $I_{\hat{W}_{25}}$ windows, together with full details of the contributions to the various windows from each individual exclusive mode, may be found in the original references noted above.

References

[1] G. W. Bennett, *et al.*, *Final Report of the Muon E821 Anomalous Magnetic Moment Measurement at BNL*, Phys. Rev. D bf 73, 072003 (2006) [arXiv:hep-ex/0602035].

[2] B. Abi, *et al.*, *Measurement of the Positive Muon Anomalous Magnetic Moment to 0.46 ppm*, Phys. Rev. Lett. **126**, 141801 (2021) [arXiv:2104.03281 [hep-ex]].

[3] D. P. Aguillard, *et al.*, *Measurement of the Positive Muon Anomalous Magnetic Moment to 0.20 ppm*, Phys. Rev. Lett. **131**, 161802 (2023) [arXiv:2308.06230 [hep-ex]].

[4] D. P. Aguillard, *et al.*, *Detailed report on the measurement of the positive muon anomalous magnetic moment to 0.20 ppm*, Phys. Rev. D **110**, 032009 (2024) [arXiv:2402.15410 [hep-ex]].

[5] T. Aoyama, *et al.*, *The anomalous magnetic moment of the muon in the Standard Model*, Phys. Rept. **887**, 1 (2020) arXiv:2006.04822 [hep-ph]].

[6] C. Bouchiat and L. Michel, *La résonance dans la diffusion méson π— méson π et le moment magnétique anormal du méson μ*, J. Phys. Radium **22**, 121 (1961) [doi:10.1051/jphysrad:01961002202012101]; S. J. Brodsky and E. de Rafael, *Suggested boson-lepton pair couplings and the anomalous magnetic moment of the muon*, Phys. Rev. **168**, 1620 (1968) [doi:10.1103/PhysRev.168.1620]

[7] D. Bernecker and H. B. Meyer, *Vector Correlators in Lattice QCD: Methods and applications*, Eur. Phys. J. A **47**, 148 (2011) [arXiv:1107.4388 [hep-lat]]

[8] Sz. Borsanyi, *et al.* [BMW], *Leading hadronic contribution to the muon magnetic moment from lattice QCD*, Nature **593**, 7857 (2021) [arXiv:2002.12347 [hep-lat]].

[9] F. V. Ignatov, *et al.* [CMD-3], *Measurement of the $e^+e^- \to \pi^+\pi^-$ cross section from threshold to 1.2 GeV with the CMD-3 detector*, Phys. Rev. D **109**, 112002 (2024) [arXiv:2302.08834 [hep-ex]].

[10] T. Blum, *et al.* [RBC/UKQCD], *Calculation of the hadronic vacuum polarization contribution to the muon anomalous magnetic moment*, Phys. Rev. Lett. **121**, 022003 (2018) [arXiv:1801.07224 [hep-lat]].

[11] C. Aubin, T. Blum, M. Golterman and S. Peris, *Muon anomalous magnetic moment with staggered fermions: Is the lattice spacing small enough?*, Phys. Rev. D **106**, 054503 (2022) arXiv:2204.12256 [hep-ph]].

[12] D. Boito, M. Golterman, K. Maltman and S. Peris, *Spectral-weight sum rules for the hadronic vacuum polarization*, Phys. Rev. D **107**, 034512 (2023) [arXiv:2210.13677 [hep-ph]].

[13] D. Boito, *et al.*, *Strong coupling from $e^+e^- \to$ hadrons below charm*, Phys. Rev. D **98**, 074030 (2018) [arXiv:1805.08176 [hep-ph]]

[14] D. Boito, *et al.*, *Strong coupling from an improved τ vector isovector spectral function*, Phys. Rev. D **103**, 034028 (2021) [arXiv:2012.10440 [hep-ph]].

[15] A. Keshavarzi, D. Nomura and T. Teubner, *The $g-2$ of charged leptons, $\alpha(M_Z^2)$ and the hyperfine splitting of muonium*, Phys. Rev. D **101**, 014029 (2020) [arXiv:1911.00367 [hep-ph]].

[16] M. Davier, A. Hoecker, B. Malaescu and Z. Q. Zhang, *A new evaluation of the hadronic vacuum polarisation contributions to the muon anomalous magnetic moment and to $\alpha(\mathbf{m_Z^2})$*,Eur. Phys. J. C **80**, 241 (2020); *erratum: ibid.* **80**, *410 (2020)* [arXiv:1908.00921 [hep-ph]].

[17] D. Boito, M. Golterman, K. Maltman and S. Peris, *Evaluation of the three-flavor quark-disconnected contribution to the muon anomalous magnetic moment from experimental data*, Phys. Rev. D **105**, 093003 (2022) [arXiv:2203.05070 [hep-ph]].

[18] J. P. Lees, *et al.*, *Measurement of the spectral function for the $\tau^- \to K^- K_S \nu_\tau$ decay*, Phys. Rev. D **98**, 032010 (2018) [arXiv:1806.10280 phep-ex]].

[19] G. Benton, *et al.*, *Data-driven estimates for light-quark-connected and strange-plus-disconnected hadronic g-2 window quantities*, Phys. Rev. D **109**, 036010 (2024) [arXiv:2311.09523 [hep-ph]].

[20] B. Aubert, *et al.*, *Measurements of $e^+e^- \to K^+K^-\eta$, $K^+K^-\pi^0$ and $K_s^0K^\pm\pi^\mp$ cross- sections using initial state radiation events*, Phys. Rev. D **77**, 092002 (2008) [arXiv:0710.4451 [hep-ex]].

[21] G. Colangelo, *et al.*, *Isospin-breaking effects in the two-pion contribution to hadronic vacuum polarization*, JHEP **10**, 032 (2022) [arXiv:2208.08993 [hep-ph]].

[22] M. Hoferichter, B. L. Hoid, B. Kubis and D. Schuh, *Isospin-breaking effects in the three-pion contribution to hadronic vacuum polarization*, JHEP **08**, 208 (2023) [arXiv:2307.02546 [hep-ph]].

[23] M. Hoferichter, *et al.*, *Phenomenological Estimate of Isospin Breaking in Hadronic Vacuum Polarization*, Phys. Rev. Lett. **131**, 161905 (2023) [arXiv:2307.02532 [hep-ph]].

[24] D. Boito, M. Golterman, K. Maltman and S. Peris, *Data-based determination of the isospin-limit light-quark-connected contribution to the anomalous magnetic moment of the muon*, Phys. Rev. D **107**, 074001 (2023) [arXiv:2211.11055 [hep-ph]].

[25] G. Benton, *et al.*, *Data-Driven Determination of the Light-Quark Connected Component of the Intermediate-Window Contribution to the Muon g-2*, Phys. Rev. Lett. **131**, 251803 (2023) [arXiv:2306.16808 [hep-ph]].

[26] G. Benton, *et al.*, *Data-driven results for light-quark connected and strange-plus-disconnected hadronic g − 2 short- and long-distance windows*, Phys. Rev. D **111**, 034018 (2025) [arXiv:2411.06637 [hep-ph]].

[27] T. Blum, *et al.* [RBC/UKQCD], *Calculation of the hadronic vacuum polarization disconnected contribution to the muon anomalous magnetic moment*, Phys. Rev. Lett. **116**, 232002 (2016) [arXiv:1512.09054 [hep-lat]].

[28] Sz. Borsanyi, *et al.* [BMW], *Hadronic vacuum polarization contribution to the anomalous magnetic moments of leptons from first principles*, Phys. Rev. Lett. **121**, 022002 (2018) [arXiv:1711.04980 [hep-lat]].

[29] D. Giusti, F. Sanfilippo and S. Simula, *Light-quark contribution to the leading hadronic vacuum polarization term of the muon g − 2 from twisted-mass fermions*, Phys. Rev. D **98**, 114504 (2018) [arXiv:1808.00887 [hep-lat]].

[30] D. Giusti, *et al.*, *HVP contribution of the light quarks to the muon* $(g-2)$ *including isospin-breaking corrections with Twisted-Mass fermions*, PoS **LATTICE2018**, 140 (2018) [arXiv:1810.05880 [hep-lat]].

[31] E. Shintani and Y. Kuramashi, *Study of systematic uncertainties in hadronic vacuum polarization contribution to muon g − 2 with 2+1 flavor lattice QCD*, Phys. Rev. D **100**, 034517 (2019) [arXiv:1902.00885 [hep-lat]].

[32] C. T. H. Davies, *et al.* [Fermilab Lattice, HPQCD, MILC], *Hadronic-vacuum-polarization contribution to the muon's anomalous magnetic moment from four-flavor lattice QCD*, Phys. Rev. D **101**, 034512 (2020) [arXiv:1902.04223 [hep-lat]].

[33] A. Gérardin, *et al.*, *The leading hadronic contribution to* $(g-2)_\mu$ *fromlattice QCD with* $N_{\rm f} = 2+1$ *flavours of O(a)improved Wilson quarks*, Phys. Rev. D **100**, 014510 (2019) [arXiv:1904.03120 [hep-lat]].

[34] C. Lehner and A. S. Meyer, *Consistency of hadronic vacuum polarization between lattice QCD and the R-ratio*, Phys. Rev D **101**, 074515 (2020) [arXiv:2003.04177 [hep-lat]].

[35] G. Wang, T. Draper, K. F. Liu and Y. B. Yang, *Muon g-2 with overlap valence fermions*, Phys. Rev. D **107**, 034513 (2023) [arXiv:2204.01280 [hep-lat]].

[36] M. Cé, *et al.*, *Window observable for the hadronic vacuum polarization contribution to the muon g − 2 from lattice QCD*, Phys. Rev. D **106**, 114502 (2022) [arXiv:2206.06582 [hep-lat]].

[37] C. Alexandrou, *et al.* [ETM], *Lattice calculation of the short and intermediate time-distance hadronic vacuum polarization contributions to the muon magnetic moment using twisted-mass fermions*, Phys. Rev. D **107**, 074506 (2023) [arXiv:2206.15084 [hep-lat]].

[38] A. Bazavov, *et al.* [Fermilab Lattice, HPQCD, MILC], *Light-quark connected intermediate-window contributions to the muon g-2 hadronic vacuum polarization from lattice QCD*, Phys. Rev. D **107**, 114514 (2023) [arXiv:2301.08274 [hep-lat]].

[39] T. Blum, *et al.* [RBC/UKQCD], *Update of Euclidean windows of the hadronic vacuum polarization*, Phys. Rev. D **108**, 054507 (2023) [arXiv:2301.08696 [hep-lat]].

[40] S. Kuberski, *et al.*, *Hadronic vacuum polarization in the muon g − 2: the short-distance contribution from lattice QCD*, JHEP **03**, 172 (2024) [arXiv:2401.11895 [hep-lat]].

[41] A. Boccaletti, *et al.*, *High precision calculation of the hadronic vacuum polarisation contribution to the muon anomaly*, arXiv:2407.10913 [hep-lat].

[42] S. Spiegel and C. Lehner, *A high-precision continuum limit study of the HVP short-distance window*, Phys. Rev. D **111**, 114517 (2025) [arXiv:2410.17053 [hep-lat]].

[43] T. Blum, *et al.* [RBC/UKQCD], *The long-distance window of the hadronic vacuum polarization for the muon g-2*, Phys. Rev. Lett. **134** 201901 (2025) [arXiv:2410.20590 [hep-lat]].

[44] D. Djukanovic, *et al.*, *The hadronic vacuum polarization contribution to the muon g − 2 at long distances*, JHEP **04** 098 (2025) [arXiv:2411.07969 [hep-lat]].

[45] A. Bazavov, *et al.* [Fermilab Lattice HPQCD, MILC], *Hadronic vacuum polarization for the muon g-2 from lattice QCD: Complete short and intermediate windows*, Phys. Rev. D **111** 094508 (2025) [arXiv:2411.09656 [hep-ph]].

[46] A. Bazavov, *et al.*, *Hadronic vacuum polarization for the muon g − 2 from lattice QCD: Long-distance and full light-quark connected contribution*, Phys. Rev. Lett. **135** 011901 (2025), [arXiv:2412.18491 [hep-lat]].